Tech Science Press

An Expected Patch Log Likelihood Denoising Method Based on Internal and External Image Similarity

Peng Xu and Jianwei Zhang[*]

School of Math and Statistics, Nanjing University of Information Science and Technology, Nanjing, 210044, China
[*]Corresponding Author: Jianwei Zhang. Email: zhangjw@nuist.edu.cn.

Abstract: Nonlocal property is an important feature of natural images, which means that the patch matrix formed by similar image patches is low-rank. Meanwhile, learning good image priors is of great importance for image denoising. In this paper, we combine the image self-similarity with EPLL (Expected patch log likelihood) method, and propose an EPLL denoising model based on internal and external image similarity to improve the preservation of image details. The experiment results show that the validity of our method is proved from two aspects of visual and numerical results.

Keywords: Nonlocal property; patch matrix; internal similarity; external similarity

1 Introduction

Image is one of the most important ways for people to pick up information from the surroundings. Unfortunately, due to various factors such as noise, the final image degradation phenomenon occurs, so image denoising has been a hot issue until today.

Up to now, many good denoising methods have been proposed. The proposition of a non-local filtering method [1] has landmark significance. After that, nonlocal features began to be the most extensive methods in image restoration task [2–4]. And sparse representation [5–9] is also a famous one among them. Its basic idea is to consider the image as a linear combination of atoms based on an over-complete dictionary. Then, the low-rank approximation methods [10–12] and the priori learning based methods [13–14] have attracted more and more attention. Inspired by these methods, more novel denoising methods have been proposed [15–16].

The internal similarity of image in this paper is what we call the self-similarity of image [17], which is a vital attribute of natural images. It means that there will be many similar pixels in natural images. The spatial position of similar pixels is not necessarily adjacent, but their gray value and neighborhood structure are usually similar. For the sake of self-similarity of images, we decompose the image into several small overlapping image patches. Taking Euclidean distance of image patches as the standard to measure the similarity, a group of similar image patches are extracted, and then they are vectorized one by one to form a similar image patch matrix. Because similar patches can be overlapped, this matrix usually has the property of low-rank.

The existence of external relevance of the image is due to the repetition or correlation of image information. EPLL (Expected patch log likelihood) method [18–19] is a very good example of application of the external similarity, and the basic idea of this method is to maximum the expected patch log likelihood and being close to the corrupted image at the same time. This method has shown promising experimental results.

In this paper, we propose an improved algorithm model based on EPLL, which makes full use of the

internal and external similarity of the image. This paper is organized as follows: Section 2 reviews the normal GMM model and the original EPLL algorithm. Section 3 introduces the principle of the low-rank method. Section 4 introduces the proposed method. In Section 5, we show experiment results to prove the effectiveness of our method. Section 6 makes the conclusion and put forward the directions for further research.

2 The EPLL Model

This part introduces the basic theory of EPLL model.

2.1 Gaussian Mixture Model

Because a single Gauss distribution has only one peak value, and in practical applications, many data are difficult to describe with a single peak, so people propose a Gauss mixture model to fit more complex data.

Assuming that the Gaussian mixture model consists of K Gaussian distributions, that is to say, K clusters, and then we define the GMM distribution as Eq. (1):

$$p(x) = \sum_{k=1}^{K} \pi_k N(x|\mu_k, \Sigma_k) \tag{1}$$

where

$$N(x|\mu_k, \Sigma_k) = (2\pi)^{-\frac{D}{2}} |\Sigma_k|^{-\frac{1}{2}} \exp\left(-\frac{1}{2}(x - \mu_k)^T \Sigma^{-1}(x - \mu_k)\right) \tag{2}$$

where K is the number of mixing components, π_k are mixing weights for each of the mixture and μ_k and Σ_k are the corresponding mean and covariance matrix. Moreover, π_k denotes the priori probability and $\sum_{k=1}^{K} \pi_k = 1$. Then, through a set of clean natural image patches $D = \{a_1, a_2, \cdots, a_N\}$, all these parameters are learned by Expectation Maximization algorithm and detailed algorithms can be seen in Tab. 1.

Table 1: EM algorithm for GMM

Input: Training set D, the number of Guassian components K;
Initialization: GMM parameters $\{\pi_k, \mu_k, \Sigma_k\}$;
Repeat
for $j = 1,2,\cdots,n$ do
calculate posterior probability:
$\gamma_{jk} = \frac{\pi_k N(a_j|\mu_k, \Sigma_k)}{\sum_{k=1}^{K} \pi_k N(a_j|\mu_k, \Sigma_k)}$ $(1 \le k \le K)$;
end for
for $k = 1,2,\cdots,K$ do
calculate new mean vectors: $\mu_k' = \frac{\sum_{j=1}^{n} \gamma_{jk} a_j}{\sum_{j=1}^{n} \gamma_{jk}}$;
calculate new covariance matrices:
$\Sigma_k' = \frac{\sum_{j=1}^{n} \gamma_{jk}(a_j - \mu_k')(a_j - \mu_k')^T}{\sum_{j=1}^{n} \gamma_{jk}}$;
calculate new mixing weights: $\pi_k' = \frac{1}{n}\sum_{j=1}^{n} \gamma_{jk}$;
end for
update parameters $\{\pi_k, \mu_k, \Sigma_k\}$ as $\{\pi_k', \mu_k', \Sigma_k'\}$;
Until the stop condition is satisfied;

2.2 Expected Patch Log Likelihood

The external similarity of image is a very good property. By decomposing the image into multiple overlapping images, we can learn a good priori. Under the trained prior distribution, we need to make the image patches approach a certain kind of the prior distribution. The noisy image u and certain prior lead to the following expression:

$$EPLL(u) = \sum_i logp(R_i u) \tag{3}$$

where the function of R_i is to extract i-centered patch, and $R_i u$ refers to the target patch. log means the likelihood of a patch.

Our purpose is to obtain a pure image by minimizing the cost function as the following:

$$f(u|u_0) = \frac{\lambda}{2} \|u - u_0\|^2 - EPLL(u) \tag{4}$$

where the left is the data fidelity term, and right of the model is the regularization term. Eq. (4) can be optimized easily according to the method of "Half Quadratic Splitting" [20].

3 Low-rank Image Denoising Based on Minimum Variance Estimator

The low-rank denoising method makes full use of the self-similarity of image. It can be regarded as a structured sparseness, and has achieved good performance in the field of image denoising in recent years.

As is shown in Fig. 1, we can see that when we take a group of similar images from the image and vectorize them one by one, then these vectors are combined into a matrix. This similarity leads to the high correlation of each column of the matrix, so the matrix is low-rank. After being affected by noise, the correlation is destroyed, and the rank of matrix becomes higher, so the denoising task essentially becomes how to reduce the rank of matrix containing noise. We all know that the rank of the matrix is determined by the non-zero singular values, and the change of the smaller singular values have less influence on the information contained in the matrix. Therefore, we choose to shrink the singular values of the matrix to realize the low-rank of the matrix, so as to achieve the purpose of denoising. Here, we make use of the internal similarity of image.

Figure 1: A simple illustration of the low-rank denoising method in this paper

Now we have noisy image u, let us define for each patch u_i the set Z_i of similar patches as:

$$Z_i \triangleq \left\{ j = 1, \cdots, N \quad s.t. \ \|u_i - u_j\|_2^2 \leq \varepsilon \right\} \tag{5}$$

where ε is some threshold.

Then we group a set of image vector $u_1, \cdots, u_N$ in to a matrix:

$$A = [u_1, \cdots, u_N] \tag{6}$$

Thus, the denoising task is converted to the estimation of similar patch matrices. We choose to use SVD to achieve property of low-rank:

$$A = U_u \Sigma_u V_u^T \tag{7}$$

The optimal estimate of A can be obtained by shrinking the singular values:

$$\hat{A} = U_u (\Sigma_u - SI) V_u^T \tag{8}$$

where S is a contraction operator that is inversely proportional to the singular value, and $\hat{A} = [\hat{u}_1, \cdots, \hat{u}_N]$.

4 Expected Patch Log Likelihood Denoising Method Based on Internal and External Image Similarity

As is known to all, EPLL exploits the external similarity of image. And the self-similarity of image is also a good priori knowledge, so we consider combining the two properties here.

Coupling low-rank priori, the new EPLL model can be expressed as:

$$f(u|u_0) = \frac{\lambda}{2} \|u - u_0\|^2 - \sum_i logP(R_i u) \tag{9}$$

where $logP(R_i u) = log(p_1(R_i u) \cdot p_2(R_i u))$, they represent the low-rank prior and the original prior of the EPLL algorithm, respectively.

A set of patches $\{x_i\}$ are introduced, we can solve the new model in the same way as in Eq. (4).

Then, another key point is that the maximum a posteriori probability (MAP) is needed, so we have to get $max \ (p_1(x_i) \cdot p_2(x_i))$.

In fact, prior knowledge p_1 and p_2 can both well describe the feature of the image patch $R_i u$, that is to say, the values of the maximum posterior estimate $x_{i,1}$ and $x_{i,2}$ are very accurate. So we hold the point that $p_1(R_i u)$ and $p_2(R_i u)$ can be maximized at the same time.

Under this assumption, $x_{i,1}$ can obtain an approximate Wiener filtering solution under the EPLL model:

$$x_{i,1} = \left(R_i u^n \Sigma_{j_{max}} + \frac{\mu_{j_{max}} I}{\beta} \right) / \left(\Sigma_{j_{max}} + \frac{I}{\beta} \right) \tag{10}$$

Through the minimum variance estimation of the similar patch matrix, we can finally obtain:

$$x_{i,2} = \frac{1}{n} (\hat{u}_1 + \cdots + \hat{u}_N)_i^{n+1} \tag{11}$$

where $x_{i,1}$ and $x_{i,2}$ are basically similar. However, a single prior knowledge has some limitations in describing the target data. So that we weighted sum $x_{i,1}$ and $x_{i,2}$ as the real value of x_i. Then, we can restore the image by alternating iterations:

$$x_i^{n+1} = a x_{i,1} + b x_{i,2} \tag{12}$$

$$u^{n+1} = (\lambda H^T u + \beta \Sigma_j R_j^T x_j^{n+1}) / (\lambda H^T H + \beta \Sigma_j R_j^T R_j) \tag{13}$$

where $u = HY$, H is a degradation factor and Y is a pure image.

EPLL algorithm makes the distribution of noisy image patches approach to a kind of GMM that has been trained. The more similar the distribution is, the less noise there is. This is because different images also contain repeated or similar information, which is what we call external similarity of images. At the same time, we put the low-rank information mentioned in Section 3 as a priori knowledge into the regular term of EPLL model, so that the internal and external similarity of images complement each other, which can achieve better denoising effect.

The proposed method can be implemented as the following Tab. 2.

Table 2: The proposed method

| |
|---|
| Input: Corrupted image u, penalty parameter β; |
| choose the most likely Gaussian mixing weights j_{max} for each patch $R_i u$; |
| calculate x_i^{n+1} using Eq. (12); |
| pre-estimate image u^{n+1} by Eq. (13); |
| Repeat above steps for 4 to 6 times; |

5 Experiment

In this section, we show the experimental results and make some discussion. In our experiments, the number of patches for training is 2×10^6. Then, we compare our method with the original EPLL method and also some other classical algorithms. Adding all the patches with Gaussian noise of zero mean and standard deviation $\sigma = 15$ or $\sigma = 30$. The parameters are arranged as: patch size $L = 8 \times 8$, search window $W = 40$, the threshold $\varepsilon = (32\sigma)^2/L$ for images scaled between 0 and 255, β usually takes the value $4/\sigma^2$ or $8/\sigma^2$, the contraction operator $S = \tau^2/\sigma$, Guassian components $K = 200$, the weights $a = b = 1/2$.
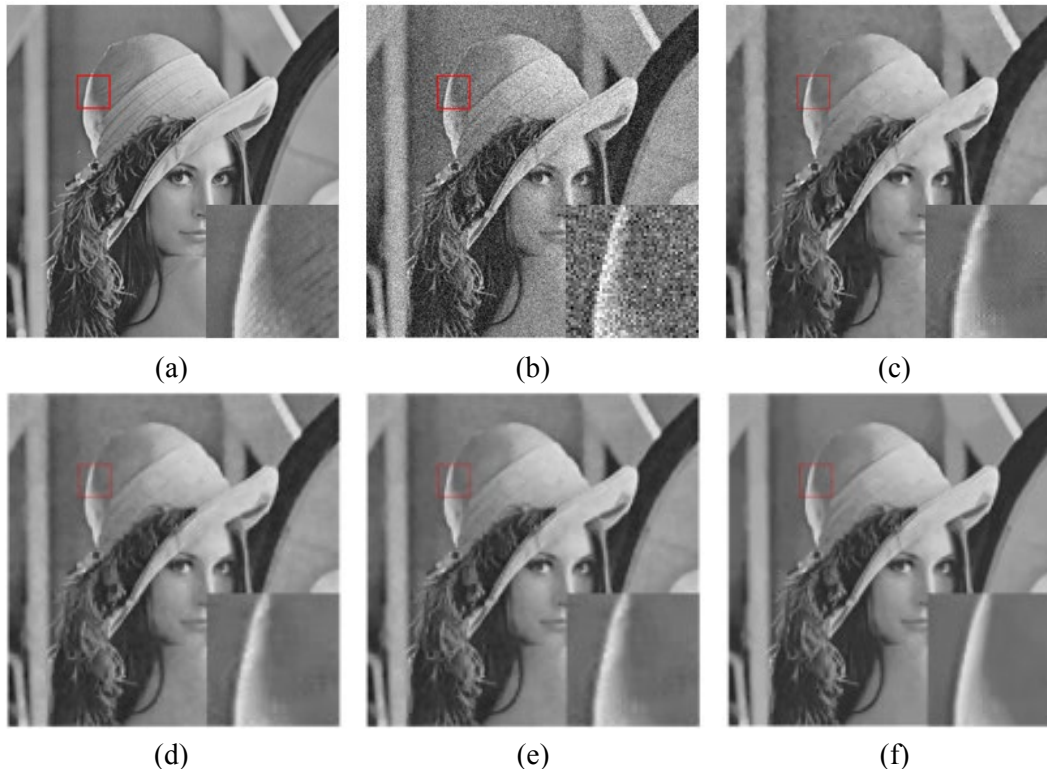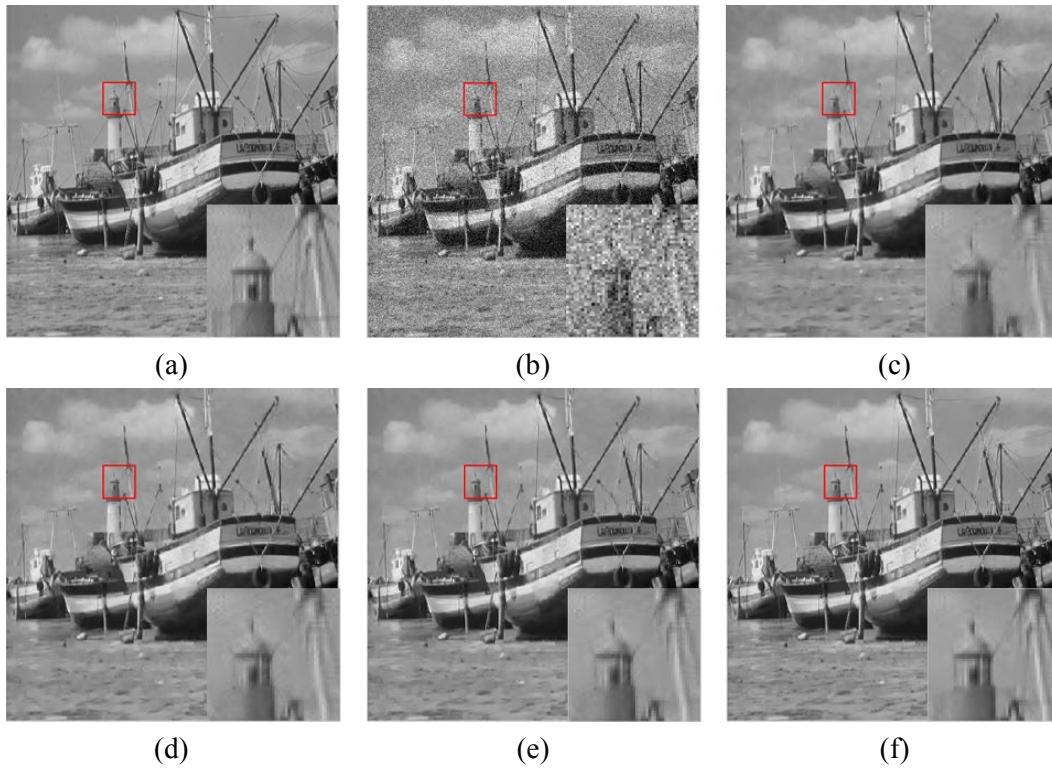

Figure 2: Denoising results on 'Lena' image with a noise standard deviation $\sigma = 30$. (a) Original image, (b) Noisy image, (c) NNM result, (d) K-SVD result, (e) EPLL result, (f)Proposed method
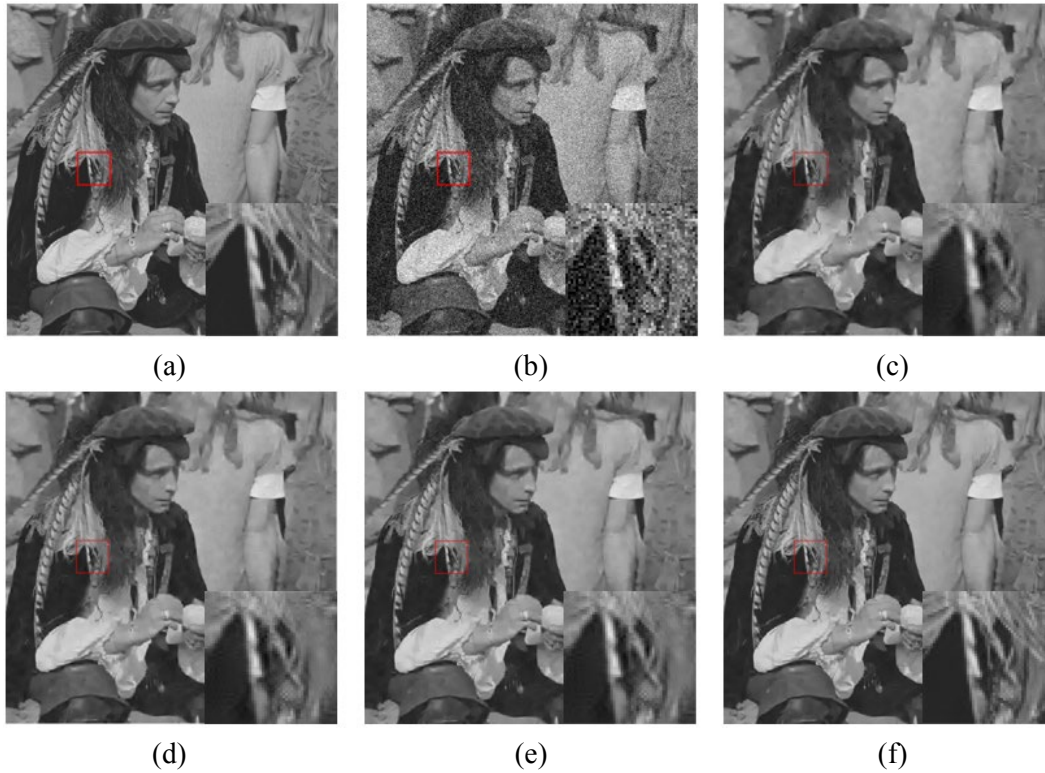
Figure 3: Denoising results on 'Man' image with a noise standard deviation $\sigma = 30$. (a) Original image, (b) Noisy image, (c) NNM result, (d) K-SVD result, (e) EPLL result, (f)Proposed method
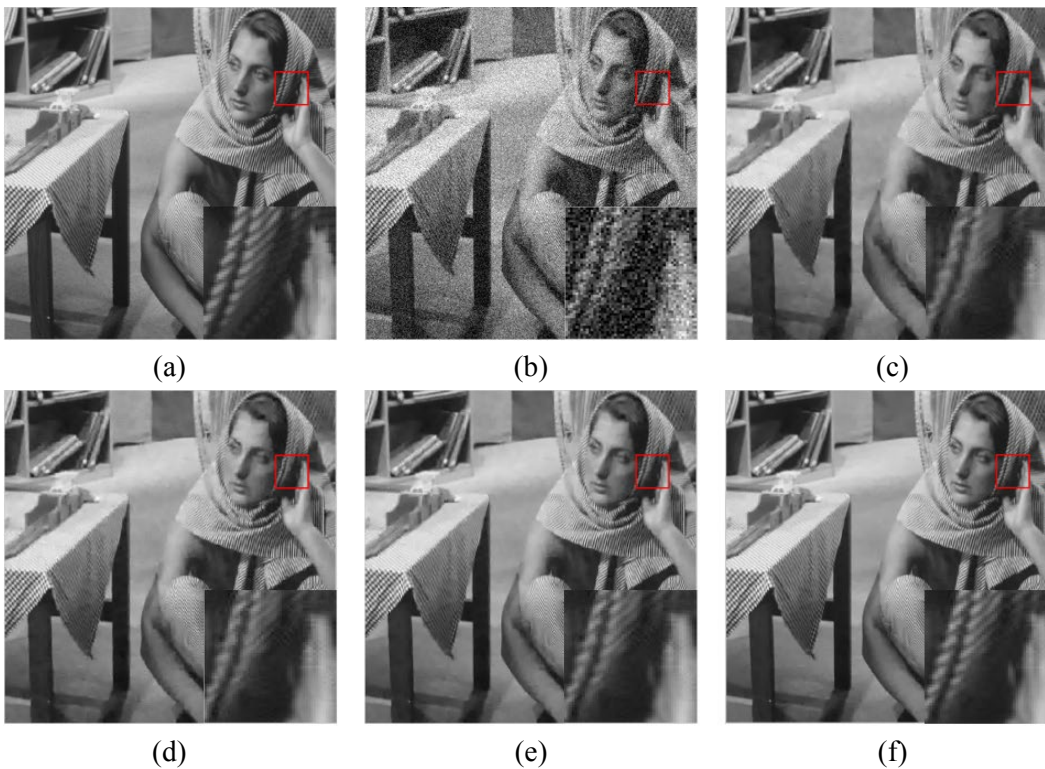
Figure 4: Denoising results on 'Barbara' image with a noise standard deviation $\sigma = 30$. (a) Original image, (b) Noisy image, (c) NNM result, (d) K-SVD result, (e) EPLL result, (f)Proposed method
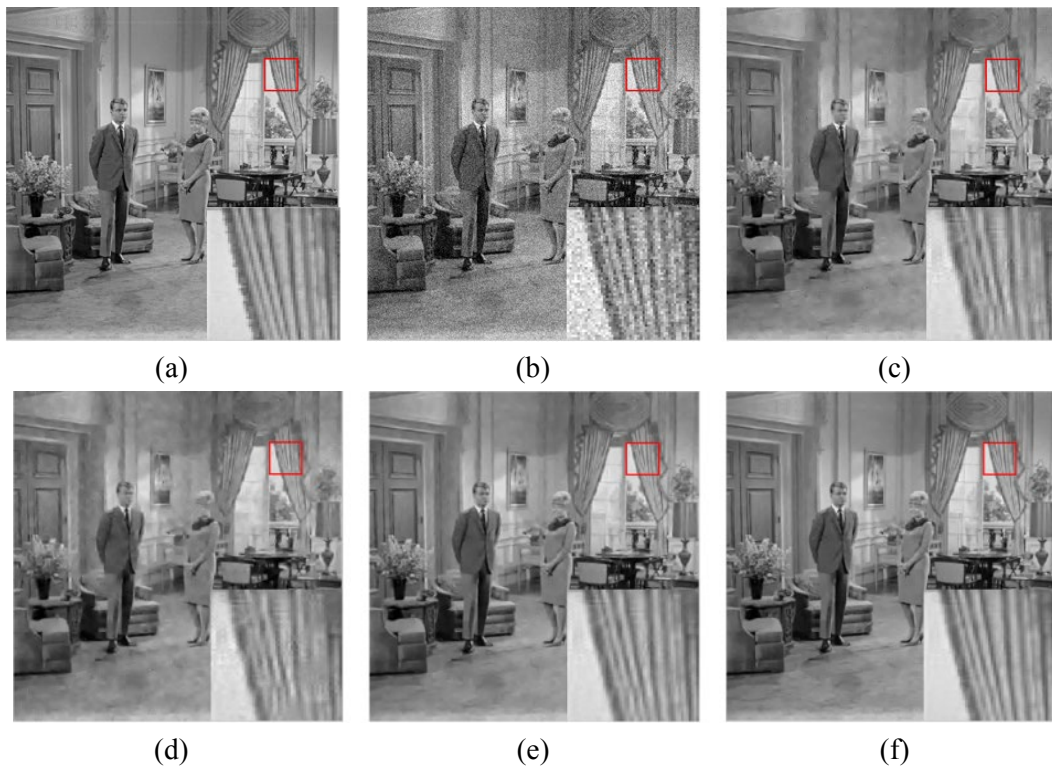
Figure 5: Denoising results on 'Boat' image with a noise standard deviation $\sigma = 30$. (a) Original image, (b) Noisy image, (c) NNM result, (d) K-SVD result, (e) EPLL result, (f)Proposed method

Figure 6: Denoising results on 'Couple' image with a noise standard deviation $\sigma = 15$. (a) Original image, (b) Noisy image, (c) NNM result, (d) K-SVD result, (e) EPLL result, (f)Proposed method

Table 3: Comparison of image denoising PSNR values

Image	Noise level	Index	KSVD	NNM	EPLL	EPLL-SGMM	Our method
Boat	$\sigma = 15$	PSNR	31.94	31.83	31.88	31.92	32.03
	$\sigma = 30$	PSNR	28.12	27.76	28.13	28.07	28.24
Hill	$\sigma = 15$	PSNR	31.42	30.97	31.58	31.42	31.56
	$\sigma = 30$	PSNR	28.33	28.04	28.65	28.51	28.73
Couple	$\sigma = 15$	PSNR	31.57	31.26	31.70	31.59	31.78
	$\sigma = 30$	PSNR	28.63	28.09	28.76	28.79	28.81
Peppers	$\sigma = 15$	PSNR	31.28	31.19	31.33	31.35	31.54
	$\sigma = 30$	PSNR	29.01	28.87	29.12	29.26	29.49
House	$\sigma = 15$	PSNR	33.77	33.06	33.94	33.87	34.15
	$\sigma = 30$	PSNR	31.16	30.85	31.19	31.23	31.42
Lena	$\sigma = 15$	PSNR	33.63	33.69	33.87	33.96	34.02
	$\sigma = 30$	PSNR	30.41	30.44	30.69	30.51	30.78
Babara	$\sigma = 15$	PSNR	31.07	29.91	31.13	31.28	31.41
	$\sigma = 30$	PSNR	27.24	27.18	27.41	27.59	27.62
Man	$\sigma = 15$	PSNR	31.39	30.98	31.52	31.44	31.67
	$\sigma = 30$	PSNR	28.26	28.07	28.43	28.29	28.82
Average	$\sigma = 15$	PSNR	31.67	31.41	32.12	31.68	32.27
	$\sigma = 30$	PSNR	28.19	27.92	29.05	28.18	29.24

As is shown in Figs. 2 to 6, compared with other methods, they still have some problems such as blurred edges and loss of regional details while our method performs well. Not only do we save the details better, the texture transition is also very natural. In Tab. 3, we use KSVD, NNM (Nuclear Norm Minimization), EPLL, EPLL-SGMM [21] and the proposed method in this paper to make a comparison. The average denoising PSNR values are calculated over all images and all noise levels for all these methods. Obviously, our method has certain advantages, and the numerical results in Tab. 3 also prove this point. This is because we combine multiple prior knowledge into one model, rather than just using a single one.

6 Conclusion

EPLL image denoising algorithm starts from the external similarity of the image, trains the Gaussian mixture model through a large number of image patches, and then makes the distribution of the noisy image patches approach to a certain type of distribution of the Gaussian mixture model. It has a certain effect, but the maintenance of the image detail texture area still needs to be improved. To solve this problem, we add a low-rank prior term to the regular term of EPLL image restoration model. The low-rank method makes use of the self-similarity of the image, through which we can know that the image also contains a lot of repeated detail texture. The matrix of similar image is approximated by SVD, and then the threshold value of the matrix is shrunk. The smaller the threshold value is, the smaller the rank is. Therefore, the preservation of the texture region by low-rank approximation promotes the restoration effect of the whole algorithm. From this point of view, coupling other prior knowledge is also worth our further study in the future.

Conflicts of Interest: The authors declare that they have no conflicts of interest to report regarding the present study.

References

[1] A. Buades, B. Coll and J. M. Morel, "Image denoising methods. A new nonlocal principle," *SIAM Review*, vol. 52, no. 1, pp. 113–147, 2010.

[2] Q. Guo, C. Zhang, Q. Liu and X. Shen, "Image interpolation based on nonlocal self-similarity," *Science Asia*, vol. 40, no. 2, pp. 168–174, 2014.

[3] B. K. S. Kumar, "Image denoising based on non-local means filter and its method noise thresholding," *Signal, Image and Video Processing*, vol. 7, no. 6, pp. 1211–1227, 2013.

[4] Z. Su, S. Zhu, X. Lv and Y. Wan, "Image restoration using structured sparse representation with a novel parametric data-adaptive transformation matrix," *Signal Processing-image Communication*, vol. 52, no. 3, pp. 151–172, 2017.

[5] M. Elad and M. Aharon, "Image denoising via sparse and redundant representations over learned dictionaries," *IEEE Transactions on Image Processing*, vol. 15, no. 12, pp. 3736–3745, 2006.

[6] K. Dabov, A. Foi, V. Katkovnik and K. Egiazarian, "Image denoising by sparse 3-d transform-domain collaborative filtering," *IEEE Transactions on Image Processing*, vol. 16, no. 8, pp. 2080–2095, 2007.

[7] M. Elad and I. Yavneh, "A plurality of sparse representation is better than the sparsest one alone," *IEEE Transactions on Information Theory*, vol. 55, no. 10, pp. 4701–4714, 2009.

[8] X. Lu, Y. Yuan and P. Yan, "Sparse coding for image denoising using spike and slab prior," *Neurocomputing*, vol. 106, no. 3, pp. 12–20, 2013.

[9] H. R. Shahdoosti and O. Khayat, "Image denoising using sparse representation classification and non-subsampled shearlet transform," *Signal, Image and Video Processing,* vol. 10, no. 6, pp. 1081–1087, 2016.

[10] J. Yang and X. Yuan, "Linearized augmented lagrangian and alternating direction methods for nuclear norm minimization," *Mathematics of Computation*, vol. 82, no. 281, pp. 301–329, 2013.

[11] B. Li, G. Lin, Q. Chen and H. Wang, "Image denoising with patch estimation and low patch-rank regularization," *Multimedia Tools and Applications*, vol. 72, no. 2, pp. 485–495, 2014.

[12] H. Wang, Y. Cen, Z. He, R. Zhao and F. Zhang, "Reweighted low-rank matrix analysis with structural smoothness for image denoising," *IEEE Transactions on Image Processing: A Publication of the IEEE Signal Processing Society*, vol. 27, no. 4, pp. 1777, 2018.

[13] R. Yan, L. Shao and Y. Liu, "Nonlocal hierarchical dictionary learning using wavelets for image denoising," *IEEE Transactions on Image Processing*, vol. 22, no. 12, pp. 4689–4698, 2013.

[14] D. Zoran and Y. Weiss, "From learning models of natural image patches to whole image restoration," *International Conference on Computer Vision*, vol. 6669, pp. 479–486, 2011.

[15] W. Dong, G. Shi, Y. Ma andX. Li, "Mage restoration via simultaneous sparse coding: where structured sparsity meets gaussian scale mixture," *International Journal of Computer Vision*, vol. 114, no. 2–3, pp. 217–232, 2015.

[16] T. Huang, W. Dong, X. Xie, G. Shi and X. Bai, "Mixed noise removal via Laplacian scale mixture modeling and nonlocal low-rank approximation," *IEEE Transactions on Image Processing*, vol. 26, no. 7, pp. 3171–3186, 2017.

[17] A. Buades, J. M. Morel and B. Coll, "Self-similarity-based image denoising," *Communication of the ACM*, vol. 54, no. 5, pp. 109–117, 2011.

[18] N. Cai, Y. Zhou, S. Wang, W. K. Ling and S. Weng, "Image denoising via patch-based adaptive gaussian mixture prior method," *Signal Image and Video Processing*, vol. 10, no. 6, pp. 1–7, 2015.

[19] C. A. Deledalle, S. Parameswaran and T. Q. Nguyen, "Image restoration with generalized gaussian mixture model patch priors," *SIAM Journal on Imaging Sciences*, vol. 11, no. 4, pp. 2568–2609, 2018.

[20] Y. Huang and D. Lu, "A preconditioned conjugate gradient method for multiplicative half-quadratic image restoration," *Applied Mathematics and Computation*, vol. 219, no. 12, pp. 6556–6564, 2013.

[21] L. Bin and L. Yuan,"EPLL based natural image restoration using spatially constrained Gaussian mixture model," *Chinese Journal of Quantum Electronics*, vol. 32, no. 4, pp. 391–398, 2015.